

STEP: Success-Rate-Aware Trajectory-Efficient Policy Optimization

Yuhan Chen¹ Yuxuan Liu² Long Zhang³ Pengzhi Gao¹ Jian Luan¹ Wei Liu^{1*}

¹MiLM Plus, Xiaomi Inc. ²Renmin University of China ³Wuhan University

{chenyuhan5, gaopengzhi, luanjian, liuwei40}@xiaomi.com
yuxuanliu@ruc.edu.cn
zlongooo@whu.edu.cn

Abstract

Multi-turn interaction remains challenging for online reinforcement learning. A common solution is trajectory-level optimization, which treats each trajectory as a single training sample. However, this approach can be inefficient and yield misleading learning signals: it applies uniform sampling across tasks regardless of difficulty, penalizes correct intermediate actions in failed trajectories, and incurs high sample-collection costs. To address these issues, we propose *STEP* (Success-rate-aware Trajectory-Efficient Policy optimization), a framework that dynamically allocates sampling based on per-task success rates and performs step-level optimization. *STEP* maintains a smoothed success-rate record to guide adaptive trajectory resampling, allocating more effort to harder tasks. It then computes success-rate-weighted advantages and decomposes trajectories into step-level samples. Finally, it applies a step-level GRPO augmentation to refine updates for low-success tasks. Experiments on OSWorld and AndroidWorld show that *STEP* substantially improves sample efficiency and training stability over trajectory-level GRPO, converging faster and generalizing better under the same sampling budget.

1 Introduction

Large language models (LLMs) have been increasingly adopted as agents for multi-turn decision-making, where they must reason, plan, and act over extended interactions with delayed and sparse rewards. Such applications include program synthesis (Zhang et al., 2024), interactive gameplay (Narasimhan et al., 2015), robotic control (Brohan et al., 2023) and GUI automation (Qin et al., 2025; Ye et al., 2025). To improve these agents’ adaptability, reinforcement learning (RL)

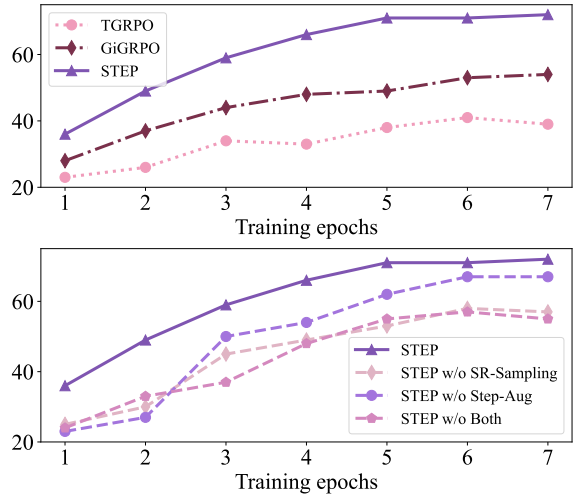


Figure 1: Number of tasks in the OSWorld training subset (128 tasks) that achieve a success rate above 60% during training across different methods. We report results for trajectory-level GRPO (T-GRPO), GiGRPO, our proposed method (*STEP*) and three ablation variants of *STEP*. Further details are provided in Section 6.2.

has become a key paradigm for online policy optimization through feedback-driven interaction.

Among RL-based methods, Group Relative Policy Optimization (GRPO) (Shao et al., 2024) has been widely adopted for its efficiency and scalability. In multi-turn settings, a common practice is to treat each trajectory—the full sequence of decisions and feedback from an episode—as a single training sample. The policy is then optimized at the trajectory level, updating parameters based on the aggregated return or relative score of the entire episode.

However, this trajectory-level formulation introduces several critical challenges:

(1) **Uniform sampling across tasks.** GRPO allocates equal sampling effort to all tasks, regardless of their difficulty or success rate. In multi-turn set-

* Corresponding author.

tings, where task complexity varies widely, this uniform allocation leads to inefficient use of the sampling budget: the agent repeatedly trains on simple, already-solved tasks while complex, low-success tasks—those that provide the most informative learning signals—receive insufficient attention.

(2) **Inaccurate credit assignment.** Multi-turn trajectories often contain a mixture of correct and incorrect actions. When the entire trajectory is treated as a single outcome, correct steps within an otherwise failed episode are penalized, propagating inaccurate gradients.

(3) **Inefficient sample collection.** Compared with single-turn scenarios, multi-turn tasks require continuous interaction with the environment. Each rollout depends heavily on environment latency, and multiple runs are needed to collect a single trajectory, making sample collection highly inefficient.

To address these challenges, we propose *STEP*(Success-rate-aware Trajectory-Efficient Policy optimization), a framework that dynamically allocates sampling and learning effort based on per-task success rates and performs fine-grained, step-level optimization. *STEP* maintains smoothed success-rate records to guide adaptive trajectory resampling, decomposes only the successful trajectories into step-level samples for success-rate-weighted credit assignment, and applies step-level GRPO augmentation for low-success tasks. This design enables both efficient use of sampling budgets and stable, high-quality learning, leading to faster convergence and better generalization in multi-turn RL scenarios.

We evaluate our approach on two general-purpose GUI benchmarks, OSWorld and Android-World, which feature complex, multi-turn interaction environments suitable for comprehensive assessment. As depicted in Figure 1, our *STEP* consistently outperforms existing methods, achieving higher efficiency and effectiveness than trajectory-level GRPO.

To sum up, we make three major contributions:

(1) We systematically analyze the challenges in multi-turn reinforcement learning and provide several key insights.

(2) Based on these insights, we propose *STEP*, a step-level training framework specifically designed for multi-turn reinforcement learning.

(3) Through extensive experiments, we demonstrate the effectiveness of *STEP*, achieving improvements both in training efficiency and performance.

2 Related Work

2.1 LLM Agents for Multi-Turn Interaction

Recent advances in Large Language Models (LLMs) (Yao et al., 2022; Brohan et al., 2023) have expanded their role from static language understanding to interactive agents that perceive, reason, and act in dynamic environments. Research has increasingly explored these agents across diverse domains, including embodied navigation in simulated homes (Shridhar et al., 2020; Li et al., 2024), multi-step web and mobile task execution leveraging structured pages and APIs (Hong et al., 2023; Gur et al., 2023; Furuta et al., 2023; Gou et al., 2024), and adaptive decision-making in interactive games (Narasimhan et al., 2015; Wang et al., 2024). A common goal across these studies is to enable LLMs to maintain coherent perception–reasoning–action loops over multiple turns, which requires robust contextual understanding and long-horizon planning. Some approaches (Schick et al., 2023; Wang et al., 2023; Zhang et al., 2023) address this by constructing modular workflows that combine multiple components to perform complex tasks, showing potential for improved performance. More recently, methods have increasingly focused on training LLMs directly on interaction data using supervised fine-tuning (SFT) (Zhang and Zhang, 2023), or reinforcement learning (RL) (Sutton and Barto, 1998), allowing models to acquire task-relevant patterns from environmental interactions.

2.2 Reinforcement Learning for Large Language Models

An early and influential application of reinforcement learning (RL) in large language models (LLMs) is RLHF (Stiennon et al., 2020; Ouyang et al., 2022), which aligns model outputs with human preferences. More recently, RL has been increasingly employed to enhance reasoning and logical deduction in LLMs, using methods such as PPO (Schulman et al., 2017), DPO (Rafailov et al., 2023), and GRPO (Shao et al., 2024). In particular, group-based RL algorithms such as GRPO, Dr. GRPO (Liu et al., 2025), and DAPO (Yu et al., 2025) have shown promise due to their low computational cost and efficient updates. By leveraging a group of samples from the same query, these methods estimate advantages without introducing an additional value function. They have achieved strong performance in tasks such as mathematical reason-

ing, search, and tool use, though these tasks are predominantly single-turn. Recent studies (Wang et al., 2025; Lu et al., 2025; Ye et al., 2025) have extended these approaches to multi-turn interactions by treating entire trajectories as sequences of independent steps. This simplification, however, overlooks the fundamental challenges inherent in multi-turn settings. One exception is GiGRPO (Feng et al., 2025), which introduces a two-level structure to estimate per-step advantages from grouped states across trajectories. Nevertheless, it focuses mainly on long-horizon training due to device constraints and does not systematically address the broader challenges of multi-turn interactions.

In this work, we first present a systematic analysis of these challenges in multi-turn RL. Building on this foundation, we propose a success-rate-guided optimization strategy that reallocates sampling resources and strengthens step-level learning signals, thereby improving both sample efficiency and policy performance of LLM agents in multi-turn interactions.

3 Preliminaries

Formally, given a task Q and an initial environment state, the LLM agent interacts with the environment over multiple steps to accomplish the task. At each step t , the agent observes a state $S_t = \langle Q, H_t, I_t \rangle$, where Q denotes the task description, H_t the interaction history, and I_t the current environment observation (e.g., a screenshot). Based on S_t , the agent generates a textual response using an LLM policy π_θ , from which an action A_t is extracted and executed in the environment, yielding an immediate reward R_t . This process continues until the episode terminates or the step limit is reached, producing a trajectory:

$$\mathcal{T} = \{\mathcal{S}_1, R_1^*, \dots, \mathcal{S}_t, R_t^*, \dots, \mathcal{S}_T, R_T\},$$

where each state-action pair $\mathcal{S}_t := (S_t, A_t)$ corresponds to step t . Here, $*$ indicates that intermediate rewards R_t^* may be unavailable in some scenarios, and R_T denotes the final trajectory reward $R_{\mathcal{T}}$. The training objective then is to update the LLM policy π_θ to maximize the expected reward across tasks.

4 Revisiting Trajectory-Level GRPO

In this section, we revisit trajectory-level group-based reinforcement learning (T-GRPO), a trajectory-focused extension of GRPO, and discuss the challenges it faces in complex multi-turn tasks.

4.1 Trajectory-Level GRPO Mechanism

Trajectory-Level GRPO is a straightforward application of GRPO to multi-turn scenarios. For a given task, the agent first samples a group of N trajectories $\mathcal{G}_{\mathcal{T}} = \{\mathcal{T}_1, \dots, \mathcal{T}_N\}$ under the old policy $\pi_{\theta_{\text{old}}}$, with each trajectory \mathcal{T} associated with a final reward R .

The trajectory advantages are then computed based on the reward statistics of the sampled group:

$$\text{Adv}(\mathcal{T}_i) = \frac{R(\mathcal{T}_i) - \text{mean}(R(\mathcal{T}_j) \mid \mathcal{T}_j \in \mathcal{G}_{\mathcal{T}})}{\text{std}(R(\mathcal{T}_j) \mid \mathcal{T}_j \in \mathcal{G}_{\mathcal{T}})}.$$

In this formulation, each state S_t within the trajectory contains the concatenation of all previous screenshots and textual responses, forming an accumulation of all past states and actions. Naturally, the trajectory \mathcal{T} is equivalent to the final state-action pair $\mathcal{S}_{\mathcal{T}}$, summarizing the agent’s entire interaction with the environment.

4.2 Challenges in T-GRPO

While effective for single-turn tasks, GRPO may encounter several challenges in complex multi-turn reasoning (T-GRPO), including: (1) Uniform sampling across tasks, (2) Misaligned learning signals, and (3) Inefficient sample collection. In the following, we discuss each of these challenges in detail.

Uniform Sampling Across Tasks Multi-turn tasks are generally more challenging, often requiring multiple epochs of training to reach satisfactory performance, which highlights the need for efficient sampling strategies. However, T-GRPO allocates an equal number of sampled trajectories to each task, without considering differences in task difficulty or success rate. This uniform allocation often results in a large portion of successful trajectories coming from simple, already-solved tasks, while challenging tasks—those that could provide more informative learning signals—receive limited attention. To systematically quantify this imbalance, we measure the proportion of high-success trajectories (success rate $> 80\%$) among all successful sampled trajectories and the result is shown in the Figure 2. We observe that this ratio remains consistently high throughout training, with the uniform sampling strategy (U-Traj)—even in the early stages—averaging around 60%. However, as shown in Figure 1, the number of high-success tasks is relatively small at the beginning of training. This suggests that under the GRPO method, the agent’s exposure to informative learning signals

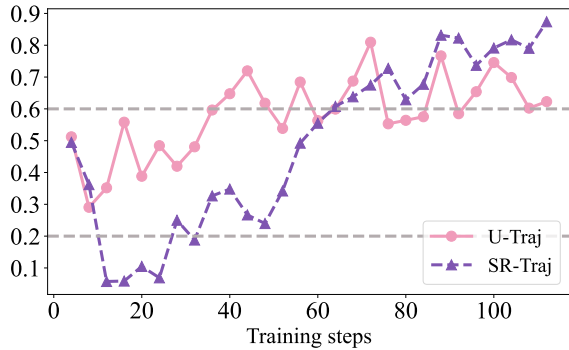
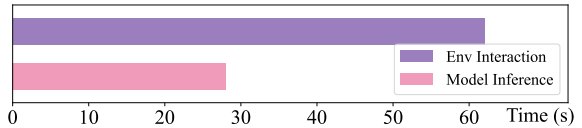


Figure 2: Proportion of high-success task trajectories over training under different sampling strategies.

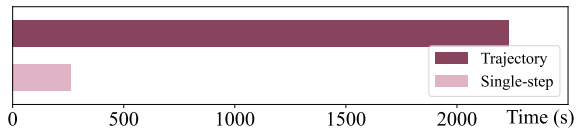
is limited in the early phase, causing it to repeatedly train on tasks it has already mastered, which can trap the model in local optima and reduce its generalization ability.

Misaligned Learning Signals T-GRPO assigns rewards solely based on the outcome of a trajectory. However, in multi-turn reasoning, a single incorrect step can invalidate the entire trajectory, even if most preceding steps are correct. We hypothesize that such coarse reward assignment overlooks valuable intermediate learning signals. To investigate this, we randomly sampled 100 failed trajectories from the OSWorld training data and manually compared their step sequences with those of successful trajectories. Surprisingly, 78% of failed trajectories contained sub-sequences identical to those in successful ones, and at the step level, the valid proportion reached 38.56%. Figures in Appendix A present representative cases from both OSWorld and AndroidWorld, where correct intermediate reasoning steps are penalized due to incorrect final predictions. These results indicate that GRPO’s trajectory-level reward fails to capture partial correctness, limiting its ability to assign credit effectively.

Inefficient Sample Collection Another critical challenge is the inefficiency of trajectory-level sampling. GRPO requires generating complete multi-turn trajectories for each training update, with each trajectory involving multiple model inferences and environment interactions. To quantify this, we measure the wall-clock time of a batch rollout of 256 trajectories and report the time per turn (Figure 3a). The results indicate that most of the time is spent on environment interactions, while model inference accounts for only a small fraction. We further compare trajectory-level and single-step sampling.



(a)



(b)

Figure 3: Analysis of sample collection efficiency. (a) Wall-clock time per turn (environment vs. model inference). (b) Sampling efficiency: trajectories vs. single steps.

To ensure a fair comparison, all turns from the trajectory-level rollouts (average trajectory length is around 15, total turns are 3,856) are re-inferred in parallel to collect timing statistics for single-step sampling. As shown in Figure 3b (b), collecting complete multi-turn trajectories is far less efficient than parallel single-step rollouts—about 8.5× slower. This bottleneck arises primarily from the high cost of environment interactions and the sequential nature of trajectory rollouts, which limits parallel inference.

From these observations, we derive the following insights:

(1) Uniform sampling wastes a significant portion of the sampling budget on already mastered tasks, hindering the learning of other valuable tasks. Sampling budgets should therefore be dynamically adjusted based on per-task success rates.

(2) Failed trajectories produce a large amount of misleading learning signals; focusing on successful trajectories can more effectively guide the model toward correct behaviors.

(3) Increasing the number of samples through parallelization—without incurring additional interaction costs with the environment—can significantly enhance sampling efficiency.

5 Method

Building upon the insights above, we introduce our method *STEP* (Success-rate-aware Trajectory-Efficient Policy optimization). As shown in the Figure 4, *STEP* adaptively adjusts both trajectory sampling and policy learning based on per-task success rates through three core components: (a) Success-rate guided trajectory sampling (SR-

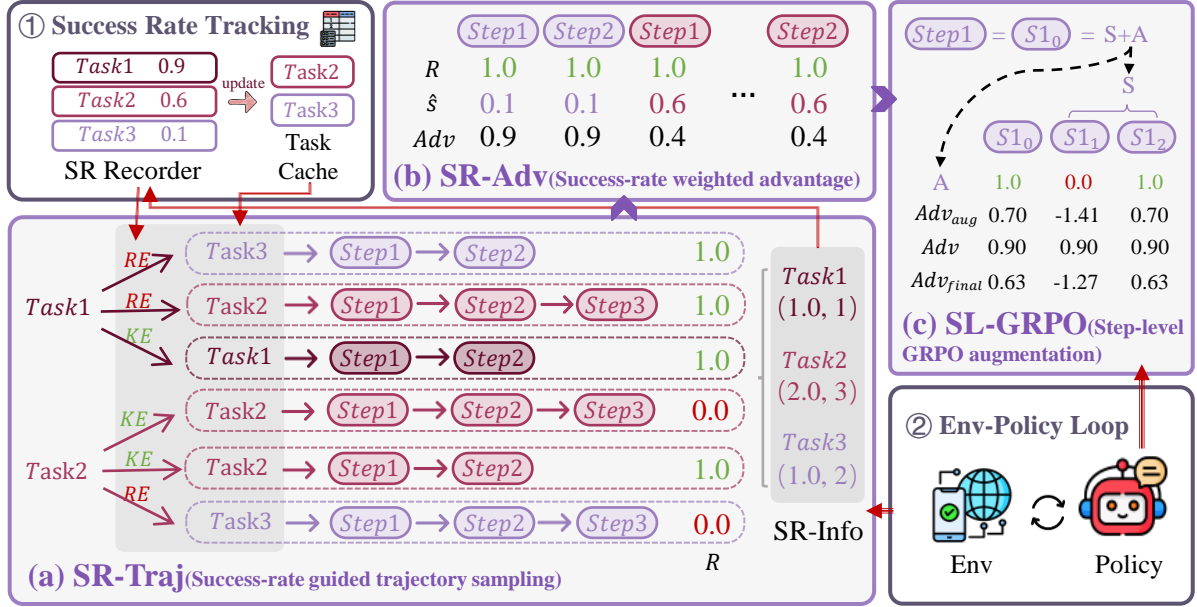


Figure 4: The framework of our STEP, which consists of three core components: (a) Success-rate guided trajectory sampling (SR-Traj, §5.1), which allocates the sampling budget based on dynamically updated success rates; (b) Success-rate weighted advantage (SR-Adv, §5.2), where we design a specific advantage function for STEP; and (c) Step-level GRPO augmentation (SL-GRPO, §5.3), which performs data augmentation without additional environment interaction costs.

Traj), (b) Success-rate weighted advantage (SR-Adv), and (c) Step-level GRPO augmentation (SL-GRPO).

5.1 Success-Rate Guided Trajectory Sampling

We propose a success-rate guided trajectory sampling strategy that dynamically reallocates sampling resources based on per-task success rates.

To track success rates, we maintain two key structures:

- **Global success-rate record** \hat{s} , which stores the estimated success rate \hat{s}_i for each task Q_i .
- **Task cache** C_Q , containing tasks with intermediate success rates ($0 < \hat{s}_i < s_0$), where s_0 is a predefined threshold.

Based on these structures, the sampling procedure is organized into two main parts: (i) Sampling Budget Reallocation and (ii) Tracking Update.

Sampling Budget Reallocation In each trajectory collection round, every task Q_i is expanded into N copies (following GRPO). For each copy¹,

¹To preserve diversity and avoid forgetting, one copy is kept; replacement is applied to the remaining $N-1$ copies.

a **replacement function** decides whether to substitute the original task with one sampled from C_Q . The replacement probability is defined by a logistic function:

$$p_{\text{rep}}(\hat{s}_i) = \frac{1}{1 + \exp(-\kappa(\hat{s}_i - s_0))},$$

where κ controls the sharpness of the transition around s_0 . So the final $\hat{Q}_{i,j}$ for the j -th copy of task Q_i is then

$$\begin{aligned} \text{rep}_{i,j} &\sim \text{Bernoulli}(p_{\text{rep}}(\hat{s}_i)), \\ \hat{Q}_{i,j} &= \begin{cases} Q_k, & \text{if } \text{rep}_{i,j} = 1, Q_k \in C_Q, \\ Q_i, & \text{otherwise.} \end{cases} \end{aligned}$$

After performing this sampling reallocation, we proceed to collect the trajectories. Intuitively, tasks with higher success rates are more likely to be replaced, thereby focusing sampling on tasks with lower success rates, which are expected to provide more informative signals.

Tracking Update In the end of each collection round, the success-rate record and cache are updated using a smoothed rule to stabilize estimates across varying sample sizes. Let N_i^τ and U_i^τ denote

the number of collected and successful trajectories for task i in the current round τ . The update is

$$\begin{aligned}\hat{s}_i^\tau &= \frac{U_i^\tau + \alpha U_i^{\tau-1}}{N_i^\tau + \alpha N_i^{\tau-1}} = \frac{U_i^\tau + \alpha \hat{s}_i^{\tau-1} N}{N_i^\tau + \alpha N}, \\ \alpha &= \begin{cases} 1 - \frac{N_i^\tau}{N}, & \text{if } N_i^\tau < N, \\ 0, & \text{otherwise,} \end{cases} \\ C_Q^\tau &= \{Q_j \mid 0 < \hat{s}_j^\tau < s_0\}.\end{aligned}$$

Here, we use an adaptive discount factor α that adjusts the influence of past estimates according to the number of collected trajectories. This design enables smooth and stable updates across rounds, preventing overly aggressive or unstable changes when data are scarce. The updated \hat{s} and C_Q are carried over to the next round for continued tracking and sampling.

5.2 Success-Rate-Weighted Advantage

After trajectory collection, we compute advantages for policy optimization. To reduce the influence of noisy or misleading signals from failed trajectories, we **use only successful trajectories**. We propose a success-rate-weighted advantage estimator that incorporates trajectory-level information and decomposes trajectories into individual steps to provide fine-grained learning signals.

Success-Rate-Weighted Trajectory Advantage
Due to the adaptive sampling strategy introduced above, different tasks yield unequal numbers of trajectories, which makes standard group-based advantage normalization unreliable. Noting that the mean reward of a task group can serve as a proxy for its success rate, we introduce a success-rate-weighted advantage, which combines each trajectory's reward with the current task success rate. For each successful trajectory $\mathcal{T}_{i,j}$ of task Q_i , the advantage is defined as

$$\text{Adv}(\mathcal{T}_{i,j}) = (1 - \hat{s}_i) \cdot R_{\mathcal{T}_{i,j}}, \quad R_{\mathcal{T}_{i,j}} > 0,$$

where \hat{s}_i denotes the smoothed success rate of task i , and $R_{\mathcal{T}_{i,j}}$ is the corresponding trajectory reward. This formulation assigns stronger learning signals to tasks with lower success rates, thereby encouraging the model to prioritize underperforming tasks.

Step-level Decomposition Each trajectory is then decomposed into step-level samples, with the same advantage assigned to all steps:

$$\text{Adv}(\mathcal{S}_{\mathcal{T},t}) = \text{Adv}(\mathcal{T}), \quad \forall t \in [1, T],$$

where $\mathcal{S}_{\mathcal{T},t}$ represents the sample at step t of the trajectory, and T is the trajectory length. Since training is performed on step-level samples, this decomposition also allows flexible organization of the history H_t within each $\mathcal{S}_{\mathcal{T},t}$ (see Section 3) using t_r past responses and t_I past observations.

5.3 Step-level GRPO Augmentation

To further improve learning efficiency and stability, we enrich the training set with valuable samples without extra environment interactions and minimal computational cost. Specifically, we selectively perform data augmentation on step samples from tasks **with low success rates** ($\hat{s}_i \leq s_{\text{low}}$), which typically correspond to steps with higher trajectory advantages.

For step samples selected from low-success trajectories, each is represented as

$$\mathcal{S} = \langle S, A, \text{Adv}(\mathcal{S}) \rangle,$$

where S denotes the state, A the action, and $\text{Adv}(\mathcal{S})$ the success-rate-weighted advantage.

To augment these samples, we expand each \mathcal{S} into a set of step-level variants by prompting the model with the same state S to generate $n = N/2 - 1$ alternative actions, where N is the group number we used in trajectory sampling; this setting balances diversity and efficiency without introducing additional hyperparameters. This **yields a group of candidate step samples**:

$$\mathcal{G}_{\mathcal{S}} = \{\mathcal{S}_k = \langle S, A_k \rangle \mid k = 0, \dots, n, A_0 = A\}.$$

The original step \mathcal{S} is thus replaced by its augmented group $\mathcal{G}_{\mathcal{S}}$, which represents localized perturbations around the original decision.

For each $\mathcal{S}_k \in \mathcal{G}_{\mathcal{S}}$, we define a step reward based on whether its action A_k **matches the reference action** A_0 . Each augmented group is then evaluated to assign relative advantages among its members:

$$\begin{aligned}R(\mathcal{S}_k) &= \begin{cases} 1, & \text{if } A_k \text{ matches } A_0, \\ 0, & \text{otherwise,} \end{cases} \\ \text{Adv}_{\text{aug}}(\mathcal{S}_k) &= \frac{R(\mathcal{S}_k) - \text{mean}(R(\mathcal{S}_j) \mid \mathcal{S}_j \in \mathcal{G}_{\mathcal{S}})}{\text{std}(R(\mathcal{S}_j) \mid \mathcal{S}_j \in \mathcal{G}_{\mathcal{S}})}.\end{aligned}$$

Finally, the step-level advantage used for policy optimization combines the trajectory-level credit and the local augmentation signal:

$$\text{Adv}_{\text{final}}(\mathcal{S}_k) = \text{Adv}(\mathcal{S}) \cdot \text{Adv}_{\text{aug}}(\mathcal{S}_k).$$

This step-level formulation encourages the policy to refine local action boundaries around high-value steps while maintaining consistency with the trajectory-level objective.

6 Experiments

6.1 Experiments Setups

Benchmarks. We selected two widely recognized benchmarks in the graphical user interface (GUI) domain—**OSWorld** (Xie et al., 2024) and **AndroidWorld** (Rawles et al., 2024). These benchmarks were chosen because they represent classical and challenging multi-turn interaction tasks in GUI-based environments, making them suitable for evaluating the robustness and generalization ability of our method. **OSWorld** provides a real-computer environment containing 369 tasks across diverse domains such as office productivity, web browsing, system management, and multi-application workflows. Following ARPO (Lu et al., 2025), we sample 128 tasks from the OSWorld benchmark as our training set. **AndroidWorld** offers a fully functional Android environment with reward signals for 116 programmatic tasks across 20 real-world Android applications. We select a subset of 43 tasks from these applications as the training set. Both benchmarks use rule-based rewards evaluated only after completing a trajectory, assigning 1.0 to successful executions and 0.0 otherwise.

Baselines and Training Details We adopt UI-Tars-DPO-7B (Qin et al., 2025) as our base model, and select (1)trajectory-level GRPO (T-GRPO) (Shao et al., 2024) and (2)GiGRPO(Feng et al., 2025)² as our baselines. Methods such as DAPO (Yu et al., 2025) or other replay-based approaches (e.g., ARPO) are excluded, as they can be integrated with our approach. All RL training methods use identical hyperparameters. The training batch size is 16, with a rollout number $N = 16$, and a PPO train size of 256. The temperature is 0.7 during training and 0 during evaluation. We apply dynamic batch updates in our method and GiGRPO, as both decompose trajectories into step-level sample, resulting in a variable number of step samples. For each step sample, the number of history responses t_r and screenshots t_I in H_t are 3 and

²In the complex GUI scenario, step-level state clustering in GiGRPO is not suitable. In this context, GiGRPO denotes a variant of GRPO in which trajectories are split into step samples, with the trajectory-level advantage distributed to each step for training.

0, respectively. The specific hyperparameters of our method are: threshold $s_0 = 0.6$, low threshold $s_{\text{low}} = 0.2$, and $\kappa = 10$. Full training settings and hyperparameters are provided in Appendix B.

6.2 Results

The overall performance on OSWorld and Android-World is summarized in Table 1, while the ablation results for *STEP*’s core components are shown in Table 2. Additionally, Figure 1 illustrates the evolution of task categories with success rates above 60% across training epochs, offering further insights into the learning dynamics.

6.2.1 Main Results

As shown in Table 1, *STEP* consistently outperforms all baselines across both benchmarks, demonstrating clear advantages on the *Train Set* and overall evaluations. On OSWorld (*Train Set*), *STEP* reaches 62.5, exceeding T-GRPO and GiGRPO by 14.1 and 7.1 points, respectively. On AndroidWorld, it achieves 45.7 overall, surpassing T-GRPO by 14.7 and GiGRPO by 11.7 points, confirming its robustness across domains.

Figure 1 further illustrates that GiGRPO and *STEP*, both using step-level samples, improve faster and achieve higher scores than T-GRPO. We hypothesize that step-level training helps reorganize trajectories and maintain shorter context windows, exposing the model to more state-similar samples and accelerating convergence. Moreover, compared with GiGRPO, *STEP* performs even better, likely due to its dynamic adjustment of in-batch training samples based on success rates. This adaptive sampling strategy encourages the model to focus on under-learned or unstable tasks, avoiding overfitting and reducing the risk of local optima. Our step-level augmentation further enriches training data by generating fine-grained samples from challenging tasks, providing higher-quality learning signals and faster convergence.

It is worth noting that the improvement from the *Train Set* to overall evaluation is less consistent on OSWorld than on AndroidWorld. On OSWorld, *STEP* improves by 21.1 points on the *Train Set* and by 7.0 points overall, whereas on AndroidWorld, the improvements are 17.8 and 16.0 points, respectively. This indicates that improvements observed during OSWorld training do not fully transfer to the overall evaluation. We hypothesize that this discrepancy stems from the OSWorld *Train Set* being constructed via pre-sampling (Lu et al., 2025),

Method	OSWorld (<i>Train Set</i>)	OSWorld	AndroidWorld (<i>Train Set</i>)	AndroidWorld
UI-Tars-DPO-7B	41.4	16.8	29.8	29.7
+ T-GRPO	48.4 (+7.0)	18.9 (+2.1)	33.3 (+3.5)	31.0 (+1.3)
+ GiGRPO	55.4 (+14.0)	21.1 (+4.3)	39.2 (+9.4)	34.0 (+4.3)
+ STEP (Ours)	62.5 (+21.1)	23.8 (+7.0)	47.6 (+17.8)	45.7 (+16.0)

Table 1: Results on OSWorld and AndroidWorld. The leading results are highlighted with **bold fonts**. Our *STEP* demonstrates superior performance in both benchmarks.

Method	OSWorld (<i>Train Set</i>)	OSWorld
STEP (Ours)	62.5	23.8
w/o SR-Sampling	57.0 (-5.5)	21.7 (-1.1)
w/o Step-Aug	60.1 (-2.4)	23.0 (-0.8)
w/o Both	56.2 (-6.3)	21.4 (-1.4)

Table 2: The results of the ablation study.

which selects tasks more likely to yield rewards. As a result, the remaining tasks in the overall set are harder and less aligned with the training distribution, leading to weaker generalization. In contrast, the AndroidWorld *Train Set* was randomly sampled, ensuring each app contributes at least one task, which allows overall performance to better reflect *Train Set* gains.

6.2.2 Ablation Study

We conduct ablation experiments to assess the contribution of each core component in *STEP*. Three variants are evaluated: (1) w/o SR-Sampling, which removes success-rate sampling; (2) w/o Step-Aug, which removes step augmentation; (3) w/o Both, which disables both components, leaving only our advantage estimation applied to GiGRPO.

As shown in Table 2, removing either SR-Sampling or Step-Aug results in a clear performance drop, demonstrating that both components are essential to the effectiveness of *STEP*. Specifically, excluding SR-Sampling causes a 7.1-point decrease on the *Train Set*, suggesting that adaptive sampling plays a key role in stabilizing training and improving sample quality. Meanwhile, as shown in Figure 1, removing Step-Aug slows down the growth in task diversity, indicating that augmenting intermediate steps provides additional supervision signals that enhance learning efficiency. The variant without both components (21.4 on OSWorld) performs slightly better than GiGRPO (23.8). This result suggests that our advantage estimation is reasonable and that training solely on successful

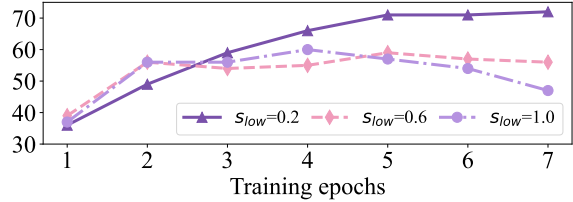


Figure 5: Number of tasks in OSWorld training subset (128 tasks) with a success rate above 60% during training across different s_{low} based on our *STEP*.

trajectories indeed provides measurable benefits.

7 Discussion

7.1 Mitigating Over-Sampling of Mastered Tasks

Uniform task sampling (U-Traj, used in T-GRPO and GiGRPO) tends to over-train on high-success tasks. In contrast, our method, Success-Rate Guided Trajectory Sampling (SR-Traj), addresses this imbalance by adjusting the sampling budget based on the dynamic task success rates. To evaluate this effect, we track the proportion of trajectories from high-success tasks ($\hat{s}_i \geq 0.8$) during training, computing the average proportion every four training steps. Figure 2 visualizes these trends, providing a direct comparison of how U-Traj and SR-Traj handle mastered tasks over time.

Results As shown in Figure 2, SR-Traj substantially reduces the proportion of high-success trajectories early in training (below 0.2), providing more opportunities to explore less-mastered tasks and generating a richer set of informative samples. As training progresses, this proportion increases, reflecting the overall improvement in task success rates. This dynamic pattern indicates that, given the same sampling budget, SR-Traj effectively mitigates premature overfitting to easier tasks, supporting more efficient learning and robust generalization in later stages.

Method	Time (min/step)	Speedup
T-GRPO	45.67	1.0x
GiGRPO	24.59	1.86x
Our <i>STEP</i>	26.25	1.74x

Table 3: Average training time per step for different methods.

7.2 Effect of Success-Rate Threshold on Step Augmentation

As mentioned previously, we applied step augmentation to tasks with low success rates ($s_{low} = 0.2$). To further verify the effect of this design, we conducted experiments by applying augmentation to tasks under different success-rate thresholds (0.2, 0.6 and 1.0). We track the evolution of task categories with success rates above 60% across training epochs according to the main experiments. The results are present in Figure 5.

Results As illustrated in the figure, all settings exhibit a rapid improvement in the early stages of training, confirming that step augmentation serves as an effective approach to accelerate model learning. However, the growth trends for higher thresholds (both 0.6 and 1.0) slow down noticeably and even decline in later stages, suggesting that applying augmentation to a broader range of tasks may suppress the learning signals from low-success tasks, thereby slightly reducing the model’s generalization ability.

7.3 Training Efficiency

We evaluate training efficiency by measuring the average time per training step. The efficiency experiments are conducted on OSWorld, where we deploy a unified setup of 16 GPUs across two nodes. The environments are simulated on a remote server with 128 parallel instances.

Results Table 3 summarizes the results. Both GiGRPO and our *STEP* substantially speed up training, achieving 1.86x and 1.74x faster steps, respectively, nearly halving the time compared to T-GRPO. We attribute this improvement to the substantial shortening of context length in both methods, which reduces inference and training overhead. Remarkably, our method retains high efficiency despite the extra cost of step augmentation during sampling. This is likely due to the avoidance of environment interaction overhead and the efficient parallel inference enabled by step rollout.

8 Conclusion

In this paper, we systematically analyze the challenges of multi-turn reinforcement learning, including uniform task sampling, inaccurate credit assignment, and inefficient sample collection. To address these issues, we propose *STEP* (Success-rate-aware Trajectory-Efficient Policy Optimization), which maintains smoothed per-task success rates to guide adaptive trajectory resampling, decomposes trajectories into step-level samples with success-rate-weighted advantages, and applies step-level GRPO augmentation to improve learning on low-success tasks. Extensive experiments demonstrate that *STEP* substantially outperforms trajectory-level GRPO in both efficiency and effectiveness. As agents face increasingly complex environments, reinforcement learning methods must evolve accordingly. For multi-turn scenarios, we envision *STEP* as a step-level framework that can serve as a foundation and reference point, offering insights for future research in efficient and adaptive multi-turn RL.

Limitations

Our method improves efficiency and performance compared to GRPO by filtering out failed trajectories and distributing trajectory rewards across all steps of successful ones. However, since failed trajectories are entirely discarded, potentially valuable sub-trajectories within them remain unused, leading to a waste of sampling resources. Moreover, even successful trajectories may contain sub-optimal or ineffective actions. These observations indicate that the current reward assignment in multi-turn scenarios remains coarse-grained. Future work could explore more fine-grained, step-level reward mechanisms that selectively leverage informative segments from both successful and partially successful trajectories to further enhance learning stability and accuracy.

References

Anthony Brohan, Noah Brown, Justice Carbajal, Yevgen Chebotar, Krzysztof Choromanski, Tianli Ding, Danny Driess, Kumar Avinava Dubey, Chelsea Finn, Peter R. Florence, Chuyuan Fu, Montse Gonzalez Arenas, Keerthana Gopalakrishnan, Kehang Han, Karol Hausman, Alexander Herzog, Jasmine Hsu, Brian Ichter, Alex Irpan, Nikhil J. Joshi, Ryan C. Julian, Dmitry Kalashnikov, Yuheng Kuang, Isabel Leal, Sergey Levine, Henryk Michalewski, Igor Mordatch, Karl Pertsch, Kanishka Rao, Krista Reymann,

Michael S. Ryoo, Grecia Salazar, Pannag R. Sanketi, Pierre Sermanet, Jaspiar Singh, Anikait Singh, Radu Soricut, Huong Tran, Vincent Vanhoucke, Quan Ho Vuong, Ayzaan Wahid, Stefan Welker, Paul Wohlhart, Ted Xiao, Tianhe Yu, and Brianna Zitkovich. 2023. [Rt-2: Vision-language-action models transfer web knowledge to robotic control](#). *ArXiv*, abs/2307.15818.

Lang Feng, Zhenghai Xue, Tingcong Liu, and Bo An. 2025. [Group-in-group policy optimization for llm agent training](#). *ArXiv*, abs/2505.10978.

Hiroki Furuta, Ofir Nachum, Kuang-Huei Lee, Yutaka Matsuo, Shixiang Shane Gu, and Izzeddin Gur. 2023. [Multimodal web navigation with instruction-finetuned foundation models](#). *ArXiv*, abs/2305.11854.

Boyu Gou, Ruohan Wang, Boyuan Zheng, Yanan Xie, Cheng Chang, Yiheng Shu, Huan Sun, and Yu Su. 2024. [Navigating the digital world as humans do: Universal visual grounding for gui agents](#). *ArXiv*, abs/2410.05243.

Izzeddin Gur, Hiroki Furuta, Austin Huang, Mustafa Safdari, Yutaka Matsuo, Douglas Eck, and Aleksandra Faust. 2023. [A real-world webagent with planning, long context understanding, and program synthesis](#). *ArXiv*, abs/2307.12856.

Wenyi Hong, Weihan Wang, Qingsong Lv, Jiazheng Xu, Wenmeng Yu, Junhui Ji, Yan Wang, Zihan Wang, Yuxiao Dong, Ming Ding, and Jie Tang. 2023. [Cogagent: A visual language model for gui agents](#). *2024 IEEE/CVF Conference on Computer Vision and Pattern Recognition (CVPR)*, pages 14281–14290.

Manling Li, Shiyu Zhao, Qineng Wang, Kangrui Wang, Yu Zhou, Sanjana Srivastava, Cem Gokmen, Tony Lee, Li Erran Li, Ruohan Zhang, Weiyu Liu, Percy Liang, Fei-Fei Li, Jiayuan Mao, and Jiajun Wu. 2024. [Embodied agent interface: Benchmarking llms for embodied decision making](#). *ArXiv*, abs/2410.07166.

Zi-Yan Liu, Changyu Chen, Wenjun Li, Penghui Qi, Tianyu Pang, Chao Du, Wee Sun Lee, and Min Lin. 2025. [Understanding r1-zero-like training: A critical perspective](#). *ArXiv*, abs/2503.20783.

Fanbin Lu, Zhisheng Zhong, Shu Liu, Chi-Wing Fu, and Jiaya Jia. 2025. [Arpo: end-to-end policy optimization for gui agents with experience replay](#). *ArXiv*, abs/2505.16282.

Karthik Narasimhan, Tejas D. Kulkarni, and Regina Barzilay. 2015. [Language understanding for text-based games using deep reinforcement learning](#). In *Conference on Empirical Methods in Natural Language Processing*.

Long Ouyang, Jeff Wu, Xu Jiang, Diogo Almeida, Carroll L. Wainwright, Pamela Mishkin, Chong Zhang, Sandhini Agarwal, Katarina Slama, Alex Ray, John Schulman, Jacob Hilton, Fraser Kelton, Luke E. Miller, Maddie Simens, Amanda Askell, Peter Welinder, Paul Francis Christiano, Jan Leike, and Ryan J. Lowe. 2022. [Training language models to follow instructions with human feedback](#). *ArXiv*, abs/2203.02155.

Yujia Qin, Yining Ye, Junjie Fang, Haoming Wang, Shihao Liang, Shizuo Tian, Junda Zhang, Jiahao Li, Yunxin Li, Shijue Huang, Wanjun Zhong, Kuanye Li, Jiale Yang, Yu Miao, Woyu Lin, Longxiang Liu, Xu Jiang, Qianli Ma, Jingyu Li, Xiaojun Xiao, Kai Cai, Chuang Li, Yaowei Zheng, Chaolin Jin, Chen Li, Xiao Zhou, Minchao Wang, Haolin Chen, Zhaojian Li, Haihua Yang, Hai-Yi Liu, Feng Lin, Tao Peng, Xin Liu, and Guang Shi. 2025. [Ui-tars: Pioneering automated gui interaction with native agents](#). *ArXiv*, abs/2501.12326.

Rafael Rafailov, Archit Sharma, Eric Mitchell, Stefano Ermon, Christopher D. Manning, and Chelsea Finn. 2023. [Direct preference optimization: Your language model is secretly a reward model](#). *ArXiv*, abs/2305.18290.

Christopher Rawles, Sarah Clinckemaillie, Yifan Chang, Jonathan Waltz, Gabrielle Lau, Marybeth Fair, Alice Li, Will Bishop, Wei Li, Folawiyo Campbell-Ajala, Daniel Toyama, Robert Berry, Divya Tyamagundlu, Timothy P. Lillicrap, and Oriana Riva. 2024. [Androidworld: A dynamic benchmarking environment for autonomous agents](#). *ArXiv*, abs/2405.14573.

Timo Schick, Jane Dwivedi-Yu, Roberto Dessì, Roberta Raileanu, Maria Lomeli, Luke Zettlemoyer, Nicola Cancedda, and Thomas Scialom. 2023. [Toolformer: Language models can teach themselves to use tools](#). *ArXiv*, abs/2302.04761.

John Schulman, Filip Wolski, Prafulla Dhariwal, Alec Radford, and Oleg Klimov. 2017. [Proximal policy optimization algorithms](#). *ArXiv*, abs/1707.06347.

Zhihong Shao, Peiyi Wang, Qihao Zhu, Runxin Xu, Jun-Mei Song, Mingchuan Zhang, Y. K. Li, Yu Wu, and Daya Guo. 2024. [Deepseekmath: Pushing the limits of mathematical reasoning in open language models](#). *ArXiv*, abs/2402.03300.

Mohit Shridhar, Xingdi Yuan, Marc-Alexandre Côté, Yonatan Bisk, Adam Trischler, and Matthew J. Hausknecht. 2020. [Alfworld: Aligning text and embodied environments for interactive learning](#). *ArXiv*, abs/2010.03768.

Nisan Stiennon, Long Ouyang, Jeff Wu, Daniel M. Ziegler, Ryan J. Lowe, Chelsea Voss, Alec Radford, Dario Amodei, and Paul Christiano. 2020. [Learning to summarize from human feedback](#). *ArXiv*, abs/2009.01325.

Richard S. Sutton and Andrew G. Barto. 1998. [Reinforcement learning: An introduction](#). *IEEE Trans. Neural Networks*, 9:1054–1054.

Guanzhi Wang, Yuqi Xie, Yunfan Jiang, Ajay Mandlekar, Chaowei Xiao, Yuke Zhu, Linxi (Jim) Fan,

and Anima Anandkumar. 2023. *Voyager: An open-ended embodied agent with large language models*. *Trans. Mach. Learn. Res.*, 2024.

Junyang Wang, Haiyang Xu, Haitao Jia, Xi Zhang, Ming Yan, Weizhou Shen, Ji Zhang, Fei Huang, and Jitao Sang. 2024. *Mobile-agent-v2: Mobile device operation assistant with effective navigation via multi-agent collaboration*. *ArXiv*, abs/2406.01014.

Zihan Wang, Kangrui Wang, Qineng Wang, Pingyue Zhang, Linjie Li, Zhengyuan Yang, Kefan Yu, Minh Nhat Nguyen, Licheng Liu, Eli Gottlieb, Monica Lam, Yiping Lu, Kyunghyun Cho, Jiajun Wu, Fei-Fei Li, Lijuan Wang, Yejin Choi, and Manling Li. 2025. *Ragen: Understanding self-evolution in ILM agents via multi-turn reinforcement learning*. *ArXiv*, abs/2504.20073.

Tianbao Xie, Danyang Zhang, Jixuan Chen, Xiaochuan Li, Siheng Zhao, Ruisheng Cao, Toh Jing Hua, Zhoujun Cheng, Dongchan Shin, Fangyu Lei, Yitao Liu, Yiheng Xu, Shuyan Zhou, Silvio Savarese, Caiming Xiong, Victor Zhong, and Tao Yu. 2024. *Os-world: Benchmarking multimodal agents for open-ended tasks in real computer environments*. *ArXiv*, abs/2404.07972.

Shunyu Yao, Jeffrey Zhao, Dian Yu, Nan Du, Izhak Shafran, Karthik Narasimhan, and Yuan Cao. 2022. *React: Synergizing reasoning and acting in language models*. *ArXiv*, abs/2210.03629.

Jiabo Ye, Xi Zhang, Haiyang Xu, Haowei Liu, Junyang Wang, Zhaoqing Zhu, Ziwei Zheng, Feiyu Gao, Junjie Cao, Zhengxi Lu, Jitong Liao, Qi Zheng, Fei Huang, Jingren Zhou, and Ming Yan. 2025. *Mobile-agent-v3: Fundamental agents for gui automation*. *ArXiv*, abs/2508.15144.

Qiying Yu, Zheng Zhang, Ruofei Zhu, Yufeng Yuan, Xiaochen Zuo, Yu Yue, Tiantian Fan, Gaohong Liu, Lingjun Liu, Xin Liu, Haibin Lin, Zhiqi Lin, Bole Ma, Guangming Sheng, Yuxuan Tong, Chi Zhang, Mofan Zhang, Wang Zhang, Hang Zhu, Jinhua Zhu, Jiaze Chen, Jiangjie Chen, Chengyi Wang, Honglin Yu, Weinan Dai, Yuxuan Song, Xiang Wei, Haodong Zhou, Jingjing Liu, Wei Ma, Ya-Qin Zhang, Lin Yan, Mu Qiao, Yong-Xu Wu, and Mingxuan Wang. 2025. *Dapo: An open-source ILM reinforcement learning system at scale*. *ArXiv*, abs/2503.14476.

China. Xiaoyan Zhang, Zhao Yang, Jiaxuan Liu, Yucheng Han, Xin Chen, Zebiao Huang, Bin Fu, and Gang Yu. 2023. *Appagent: Multimodal agents as smartphone users*. *ArXiv*, abs/2312.13771.

Kechi Zhang, Jia Li, Ge Li, Xianjie Shi, and Zhi Jin. 2024. *Codeagent: Enhancing code generation with tool-integrated agent systems for real-world repo-level coding challenges*. In *Annual Meeting of the Association for Computational Linguistics*.

Zhuosheng Zhang and Aston Zhang. 2023. *You only look at screens: Multimodal chain-of-action agents*. *ArXiv*, abs/2309.11436.

A Misaligned Learning Signals in OSWorld and AndroidWorld.

We present cases of misaligned learning signals in both OSWorld and AndroidWorld. As shown in Figure 6 and Figure 7, successful and failed trajectories for the same task often share similar intermediate reasoning steps, but diverge at a critical decision point where the failed trajectory takes an incorrect action. This example illustrates that failure trajectories, although their final outcome is negative, often contain many valid intermediate steps. Penalizing the entire trajectory can lead to incorrect learning for these correct steps.

B Setting

We provide our detail settings in Table 4 and Table 5.

Hyperparameters	All methods
Train batch size	16
PPO batch size	256
Training epoches	8
Rollout numbers	16
Image tokens	1350
Temperature	0.7
Learning rate	1e-6
Kl coefficient	0.001
GPU numbers	16

Table 4: Model configurations for all methods.

Hyperparameters	T-GRPO	GiGRPO&STEP
Max turns (OSWorld)	20	30
Max turns (AndroidWorld)	20	25
Prompt length	3076	4096
Response length	29692 (256 per turn)	256

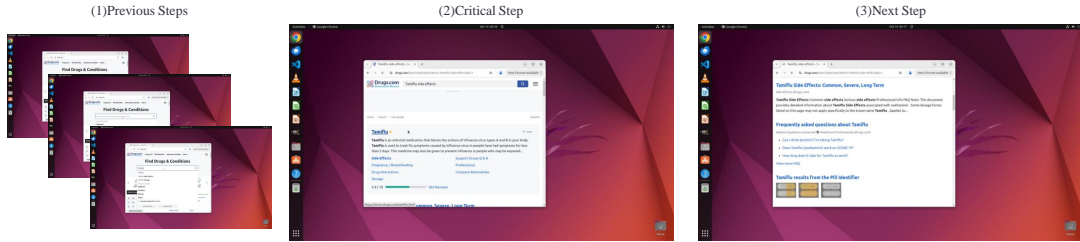
Table 5: Model configurations across methods.



Critical Action Content: Thought: To proceed with gathering detailed information about the side effects of Tamiflu, I need to click on the "Side Effects" link. This will likely lead to a more comprehensive view of the side effects, which is essential for completing the task. Click on the "Side Effects" link to access detailed information about the side effects of Tamiflu.

Critical Action: click(start_box=(235,618))

(a) Successful Trajectory

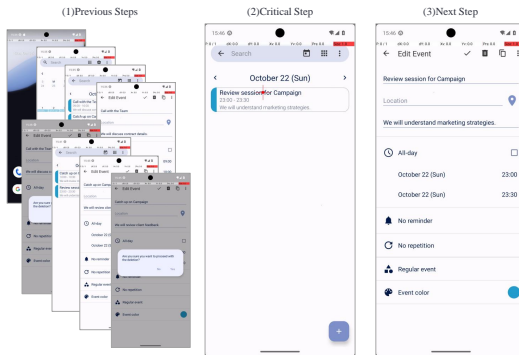


Critical Action Content: Thought: To access the complete information about the side effects of Tamiflu, I need to scroll down the page. This will allow me to view the additional content that is currently not visible, ensuring I gather all relevant details about the drug's side effects. Scroll down the page to reveal more information about the side effects of Tamiflu.

Critical Action: scroll(direction='down', start_box=(307,487))

(b) Failed Trajectory

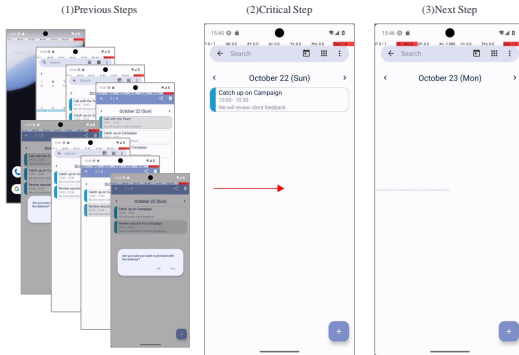
Figure 6: Comparison of success and failure trajectories in OSWorld for the task “Show side effects of Tamiflu.”



Critical Action Content: Thought: To proceed with the task of deleting all events for October 22, I need to tap on the "Review session for Campaign" event. This action will open its details, allowing me to access further options for managing or removing the event, which is a necessary step in completing the task. Tap on the "Review session for Campaign" event to open its details.

Critical Action: click(start_box=(387,206))

(a) Successful Trajectory



Critical Action Content: Thought: To ensure that all events on October 22, 2023, are reviewed and potentially deleted, I need to scroll through the page to reveal any additional events that may not currently be visible. This step is necessary to locate and manage all events scheduled for that day. Scroll the page in the up direction to display more information and reveal any additional events on October 22, 2023.

Critical Action: scroll(start_box=(65,495), end_box=(531,495))

(b) Failed Trajectory

Figure 7: Comparison of success and failure trajectories in AndoridWorld for the task “In Simple Calendar Pro, delete all the calendar events on 2023-10-22.”